

## 以 $\text{PW}_9$ 为结构基元构筑的夹心型多金属 氧酸盐化合物的合成与晶体结构

冯秀玲

(怀化学院化学与化学工程系, 怀化 418008)

**摘要:** 通过水热合成方法合成了以夹心多酸阴离子  $[\text{Ni}_4(\text{H}_2\text{O})_2(\text{PW}_9\text{O}_{34})_2]^{10-}$ , 乙二胺(en)和  $\text{Ni}(\text{II})$  构筑的夹心型多金属氧酸盐化合物  $[\text{Ni}(\text{en})_2]_2\{[\text{Ni}(\text{en})_2][\text{Ni}(\text{en})_2\text{H}_2\text{O}]\{(\text{PW}_9\text{O}_{34})_2\text{Ni}_4(\text{H}_2\text{O})_2\}\} \cdot 16\text{H}_2\text{O}$  (**1**), 采用 IR、单晶 X-射线衍射法、TG/DTG 及循环伏安法对标题化合物进行结构和性质研究。该化合物的夹心多酸阴离子通过  $[\text{Ni}(\text{en})_2]^{2+}$  连接形成一维链, 并进一步通过氢键作用形成 3D 超分子结构。

**关键词:** 多金属氧酸盐; 晶体结构; 热重分析; 电化学性能

中图分类号: O614.81+3; O614.61+3

文献标识码: A

文章编号: 1001-4861(2013)12-2603-06

DOI: 10.3969/j.issn.1001-4861.2013.00.366

## Synthesis and Crystal Structure of a Sandwich-Type Polyoxometalate Built up of the $\text{PW}_9$ Unit

FENG Xiu-Ling

(College of Chemistry and Chemical Engineering, Huaihua University, Huaihua, Hunan 418008, China)

**Abstract:** A sandwich-type polyoxometalate compound built on sandwich-type polyoxoanion  $[\text{Ni}_4(\text{H}_2\text{O})_2(\text{PW}_9\text{O}_{34})_2]^{10-}$ , ethylenediamine(en) and  $\text{Ni}(\text{II})$  cation,  $[\text{Ni}(\text{en})_2]_2\{[\text{Ni}(\text{en})_2][\text{Ni}(\text{en})_2\text{H}_2\text{O}]\{(\text{PW}_9\text{O}_{34})_2\text{Ni}_4(\text{H}_2\text{O})_2\}\} \cdot 16\text{H}_2\text{O}$  (**1**), has been hydrothermally synthesized and characterized by IR spectrum, single crystal X-ray diffraction analysis, TG /DTG and electrochemical studies. The sandwich polyoxoanions are linked by  $[\text{Ni}(\text{en})_2]^{2+}$  cations to form a 1D linear structure and the multiform hydrogen bonds in the compound form a 3D supramolecular framework. CCDC: 917320.

**Key words:** polyoxometalates; crystal structure; thermogravimetric analysis; electrochemical property

## 0 Introduction

In recent years, more and more attention has been paid to research on transitional metal-substituted polyoxometalates (TMSPs) owing to their unexpected structures and many promising properties for applications<sup>[1-4]</sup>. Within the TMSPs class, the sandwich type structures are very important in the sense that they are similar in construction to naturally occurring enzy-

mes and cofactors<sup>[5]</sup>. The known characterized structures of sandwich-type polyoxometalates can be obtained by the reaction of a transition metal ion (e.g.  $\text{Co}^{2+}$ ,  $\text{Ni}^{2+}$ ) with appropriate lacunary polyoxometalates precursor (e.g.  $[\text{AsW}_9\text{O}_{33}]^{9-}$ ,  $[\text{PW}_9\text{O}_{34}]^{9-}$  and  $[\text{P}_2\text{W}_{15}\text{O}_{56}]^{12-}$ )<sup>[6]</sup>. The incorporation of transition metals makes it possible to obtain structures with diverse chemical properties, especially remarkable catalytic activity. Numerous nickel-substituted trivacant  $\alpha$ -B Keggin polyoxome-

收稿日期: 2013-02-26。收修改稿日期: 2013-06-13。

湖南省教育厅(No.12C0839)资助项目。

E-mail: xiulingfeng2001@sina.com, Tel: 15115121472

talates with sandwich structures have been synthesized and most belong to  $[\text{Ni}(\text{H}_2\text{O})_3(\text{XW}_9\text{O}_{33})_2]^{n-}$  ( $\text{X}=\text{As}^{3+}$ ,  $\text{Sb}^{3+}$ ,  $\text{Te}^{4+}$ , etc) and  $[\text{Ni}_4(\text{H}_2\text{O})_2(\text{XW}_9\text{O}_{34})_2]^{n-}$  ( $\text{X}=\text{As}^{5+}$ ,  $\text{Si}^{4+}$ ,  $\text{Ga}^{4+}$ ,  $\text{Zn}^{2+}$ , etc) series<sup>[7-9]</sup>. We report herein the synthesis, crystal structure, and characterizations of a new compound  $[\text{Ni}(\text{en})_2]_2\{[\text{Ni}(\text{en})_2]\{\text{Ni}(\text{en})_2\text{H}_2\text{O}\}_2\{(\text{PW}_9\text{O}_{34})_2\text{Ni}_4(\text{H}_2\text{O})_2\}\cdot 16\text{H}_2\text{O}$  (**1**). In the compound, the sandwich polyoxoanions are linked by  $[\text{Ni}(\text{en})_2]^{2+}$  cations to form a 1D linear structure, which further stacks to form a 3D framework through hydrogen bonding.

## 1 Experimental

### 1.1 Materials and instruments

All the reagents were used as commercial sources without further purification. Elemental analyses were performed on an Elementary Vario EL analyzer. The IR spectra were recorded on AVATAR 360 spectrophotometer using KBr discs in the  $400\sim 4\,000\text{ cm}^{-1}$ . Thermal analyses (TGA-DTG) were performed on a STA-409PC instrument under nitrogen atmosphere with a heating rate of  $15\text{ }^\circ\text{C}$ . Electrochemical measurements were made on a CHI660b electrochemical workstation. A conventional three-electrode system was used. The working electrode was a modified carbon paste electrode (1-CPE).  $\text{Ag}/\text{AgCl}$  (3 mol  $\cdot\text{L}^{-1}$  KCl) electrode was used as a reference electrode and a Pt wire as a counter electrode.

### 1.2 Synthesis

A mixture of nickel nitrate (1 mmol),  $\text{Na}_9\text{PW}_9\text{O}_{34}$  (0.3 mmol) and ethylenediamine (1 mmol) in 15 mL

distilled water was heated at 413 K in a Teflon-lined stainless steel autoclave for three days. The reaction system was then slowly cooled to room temperature and yellow crystals of the title compound suitable for single crystal X-ray diffraction analysis were obtained (yield 40% based on W). Anal. Calcd. for  $\text{C}_{20}\text{H}_{120}\text{N}_{20}\text{Ni}_9\text{O}_{88}\text{P}_2\text{W}_{18}$  (%): C 4.03; H 2.01; N 4.71. Found (%): C 4.07; H 2.08; N 4.64.

### 1.3 Structure determination

A single crystal with dimensions of  $0.25\text{ mm}\times 0.10\text{ mm}\times 0.06\text{ mm}$  was mounted on a Bruker CCD diffractometer equipped with a graphite-monochromatic  $\text{Mo K}\alpha$  ( $\lambda=0.071\,073\text{ nm}$ ) radiation by using a  $\omega$  scan mode ( $2.50^\circ$  to  $25.02^\circ$ ) at 293(2) K. A total of 17 519 reflections were collected and 9 656 were independent with  $R_{\text{int}}=0.027\,4$ , completeness=0.999 ( $\theta=25.02^\circ$ ). The structure was solved by direct methods with SHELXS-97 program<sup>[10]</sup> and refined by full-matrix least-squares techniques on  $F^2$  with SHELXL-97<sup>[11]</sup>. All non-hydrogen atoms were refined anisotropically and hydrogen atoms isotropically. The crystallographic data are list in Table 1.

CCDC: 917320.

## 2 Results and discussion

### 2.1 Crystal structure of the compound

The molecular structure of the title complex is shown in Fig.1 and the selected bond lengths and bond angles are given in Table 2. Single crystal X-ray diffraction analysis reveals that **1** consists of a

Table 1 Crystal data and structure refinement for the complex **1**

Empirical formula	$\text{C}_{20}\text{H}_{120}\text{N}_{20}\text{Ni}_9\text{O}_{88}\text{P}_2\text{W}_{18}$	$D_c / (\text{g}\cdot\text{cm}^{-3})$	3.606
Formula weight	5 948.63	$Z$	1
Temperature / K	293(2)	Absorption coefficient / $\text{mm}^{-1}$	21.501
Crystal system	Triclinic	$F(000)$	2 772
Space group	$P\bar{1}$	Crystal size / mm	$0.25\times 0.10\times 0.06$
$a / \text{nm}$	1.317 57(4)	$\theta / (^\circ)$	2.50 to 25.02
$b / \text{nm}$	1.556 08(7)	Limiting indices	$-15\leq h\leq 15, -18\leq k\leq 18, -16\leq l\leq 18$
$c / \text{nm}$	1.563 59(6)	Reflections collected / unique ( $R_{\text{int}}$ )	17 519 / 9 656 (0.027 4)
$\alpha / (^\circ)$	112.570(4)	Refinement method	Full-matrix least-squares on $F^2$
$\beta / (^\circ)$	91.549(3)	Data / restraints / parameters	9 656 / 0 / 720
$\gamma / (^\circ)$	109.817(3)	Goodness of fit on $F^2$	1.029
$V / \text{nm}^3$	2.738 97(18)	Final $R$ indices ( $I>2\sigma(I)$ )	$R_1=0.026\,2, wR_2=0.053\,9$

Table 2 Selected bonds lengths (nm) and angles ( $^\circ$ )

W(1)-O(26)	0.173 8(5)	Ni(1)-O(24) <sup>i</sup>	0.208 1(5)	Ni(4)-N(5)	0.208 2(7)
W(1)-O(11)	0.202 4(6)	Ni(1)-O(23) <sup>i</sup>	0.208 2(5)	Ni(4)-N(3)	0.208 6(7)
W(2)-O(27)	0.171 5(6)	Ni(1)-O(35)	0.208 7(6)	Ni(4)-N(6)	0.208 7(8)
W(3)-O(28)	0.172 5(5)	Ni(1)-O(4)	0.217 7(5)	Ni(4)-N(4)	0.209 4(7)
W(4)-O(29)	0.169 8(5)	Ni(2)-O(25) <sup>i</sup>	0.200 9(5)	Ni(4)-O(36)	0.215 0(6)
W(5)-O(30)	0.172 3(6)	Ni(2)-O(22)	0.201 1(6)	Ni(4)-O(32)	0.218 3(6)
W(6)-O(31)	0.171 8(5)	Ni(2)-O(23)	0.204 7(5)	Ni(5)-N(8) <sup>vi</sup>	0.189 8(8)
W(7)-O(32)	0.173 3(6)	Ni(2)-O(24) <sup>i</sup>	0.207 3(5)	Ni(5)-N(8)	0.189 8(8)
W(8)-O(33)	0.171 8(6)	Ni(2)-O(4) <sup>i</sup>	0.216 7(5)	Ni(5)-N(7)	0.191 3(9)
W(9)-O(34)	0.171 5(5)	Ni(2)-O(4)	0.219 4(5)	Ni(5)-N(7) <sup>vi</sup>	0.191 3(9)
O(1)-P(1)	0.155 6(5)	Ni(3)-N(2) <sup>v</sup>	0.205 4(8)	Ni(6)-N(10)	0.191 2(9)
O(2)-P(1)	0.155 0(5)	Ni(3)-N(2)	0.205 4(8)	Ni(6)-N(10) <sup>vii</sup>	0.191 2(9)
O(3)-P(1)	0.155 7(5)	Ni(3)-N(1)	0.211 1(9)	Ni(6)-N(9)	0.192 2(8)
O(4)-P(1)	0.154 9(6)	Ni(3)-N(1) <sup>v</sup>	0.211 1(9)	Ni(6)-N(9) <sup>vii</sup>	0.192 2(8)
Ni(1)-O(21)	0.201 9(6)	Ni(3)-O(26) <sup>v</sup>	0.214 0(5)		
Ni(1)-O(20)	0.202 2(5)	Ni(3)-O(26)	0.214 0(5)		
O(5)-W(1)-O(11)	81.7(2)	O(4)-P(1)-O(2)	110.4(3)	O(4)i-Ni(2)-O(4)	85.5(2)
O(27)-W(2)-O(21)	105.0(3)	O(4)-P(1)-O(1)	111.7(3)	N(2)v-Ni(3)-N(1)	96.0(4)
O(28)-W(3)-O(22)	104.6(3)	O(2)-P(1)-O(1)	108.3(3)	N(2)v-Ni(3)-O(26) <sup>v</sup>	89.4(3)
O(29)-W(4)-O(23)	104.1(3)	O(4)-P(1)-O(3)	109.9(3)	O(26)v-Ni(3)-O(26)	180.000(2)
O(30)-W(5)-O(24)	103.1(3)	O(21)-Ni(1)-O(24) <sup>i</sup>	91.8(2)	N(5)-Ni(4)-N(3)	95.3(3)
O(31)-W(6)-O(25)	103.5(3)	O(20)-Ni(1)-O(23) <sup>i</sup>	90.4(2)	N(6)-Ni(4)-N(4)	99.8(3)
O(32)-W(7)-O(12)	103.2(2)	O(35)-Ni(1)-O(4)	179.0(2)	O(36)-Ni(4)-O(32)	175.2(2)
O(33)-W(8)-O(13)	101.7(2)	O(25)i-Ni(2)-O(22)	92.5(2)	N(8)vi-Ni(5)-N(7)	93.2(4)
O(34)-W(9)-O(16)	101.7(2)	O(23)-Ni(2)-O(24) <sup>i</sup>	169.1(2)	N(10)-Ni(6)-N(9)	86.9(3)

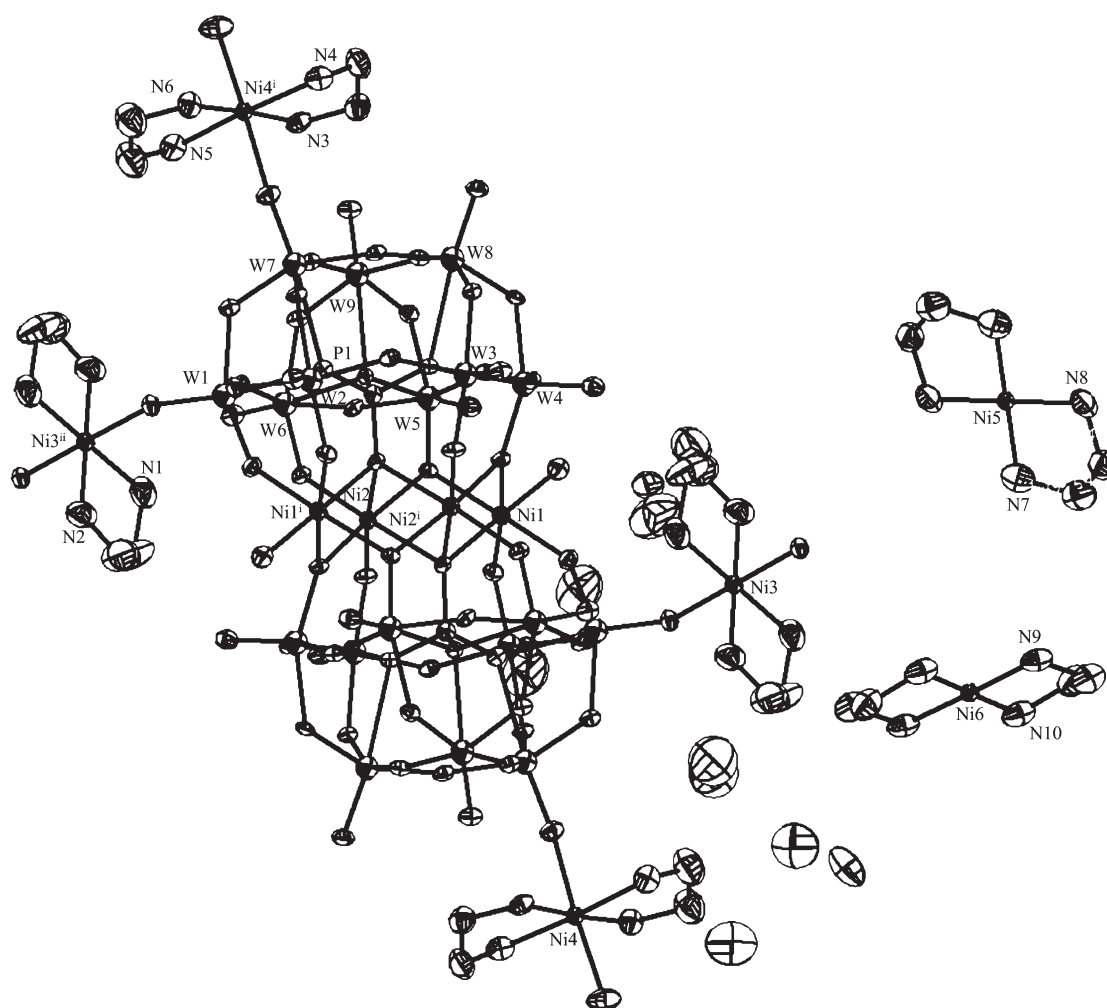
Symmetry code: <sup>i</sup> -x+1, -y+1, -z+1; <sup>v</sup> -x+1, -y+2, -z+1; <sup>vi</sup> -x+1, -y+3, -z; <sup>vii</sup> -x+2, -y+3, -z+1.

centrosymmetric polyoxoanion  $[\{\text{Ni}(\text{en})_2\text{H}_2\text{O}\}_2\{(\alpha\text{-B-PW}_9\text{O}_{34})_2\text{Ni}_4(\text{H}_2\text{O})_2\}]^{6-}$ , two isolated  $[\text{Ni}(\text{en})_2]^{2+}$  cations, one bridging  $[\text{Ni}(\text{en})_2]^{2+}$  and sixteen lattice water molecules. Two decorating  $\{\text{Ni}(\text{en})_2(\text{H}_2\text{O})\}^{2+}$  coordinate with two terminal oxygen atoms of the tetra-Ni substituted polyoxoanion  $\{(\alpha\text{-B-PW}_9\text{O}_{34})_2\text{Ni}_4(\text{H}_2\text{O})_2\}^{10-}$  and the bridging  $[\text{Ni}(\text{en})_2]^{2+}$  cations connect the adjacent polyoxoanions via terminal O into a chain motif parallel to [010] (Fig.2). The  $\{(\alpha\text{-B-PW}_9\text{O}_{34})_2\text{Ni}_4(\text{H}_2\text{O})_2\}^{10-}$  has the general structure of the series complexes reported<sup>[12]</sup> and contains two trivacant Keggin  $\{\alpha\text{-B-PW}_9\text{O}_{34}\}^{9-}$  fragments in a staggered fashion linked by a centrosymmetric unit  $\text{Ni}_4\text{O}_{16}$  group, leading to a sandwich-typed structure. The Ni centers in the  $\text{Ni}_4\text{O}_{16}$  fragment are coordinated to the fourteen O atoms of two  $\{\text{PW}_9\text{O}_{34}\}^{9-}$  units and two water O atoms. All the Ni atoms in the  $\text{Ni}_4\text{O}_{16}$  have a distorted  $\text{NiO}_6$  octahedral

environment with Ni-O (0.200 9(5)~0.219 4(5) nm) bonds in the usual range.

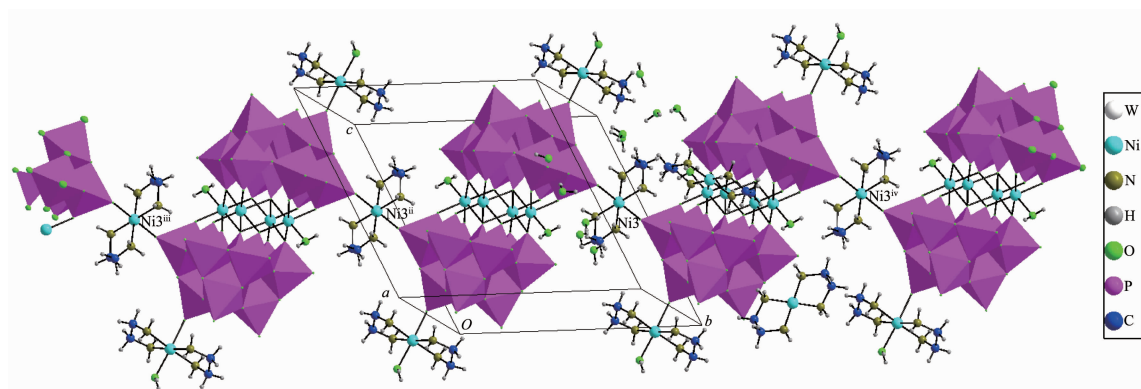
The Ni ion in the  $\{\text{Ni}(\text{en})_2(\text{H}_2\text{O})\}^{2+}$  group displays an octahedral geometry with four N atoms from two en ligands in the basal positions and the axial positions are occupied by two O atoms from polyoxoanion and water ligand (Ni-N: 0.208 2(7)~0.218 3(6) nm; Ni-O: 0.215 0(6)~0.218 3(6) nm). In the isolate  $[\text{Ni}(\text{en})_2]^{2+}$  and bridging  $[\text{Ni}(\text{en})_2]^{2+}$ , the Ni atoms lie on inversion centers and display square coordination and octahedral geometry respectively (Ni-N: 0.189 8(8)~0.211 1(9) nm; Ni-O: 0.214 0(5) nm).

The whole crystal is stabilized by double forces: electrostatic attraction and hydrogen-bonding interactions. All N atoms of en form N-H...O hydrogen bonds with O atoms of polyoxoanion and water. The water molecules form hydrogen bonding O-H...O with



All hydrogen atoms are omitted for clarity; symmetry code: <sup>i</sup>  $-x+1, -y+1, -z+1$ ; <sup>ii</sup>  $x, y-1, z$

Fig.1 Molecular structure of the complex **1** showing 50% probability displacement ellipsoids



Symmetry code: <sup>ii</sup>  $x, y-1, z$ ; <sup>iii</sup>  $x, y-2, z$ ; <sup>iv</sup>  $x, y+1, z$

Fig.2 View of the 1D chain in the complex **1**

O atoms of polyoxoanion. Besides, hydrogen bonding between water molecules also occurs (Table 3). The complex **1** forms a 3D supramolecular network through multiform hydrogen bonds.

## 2.2 IR spectra

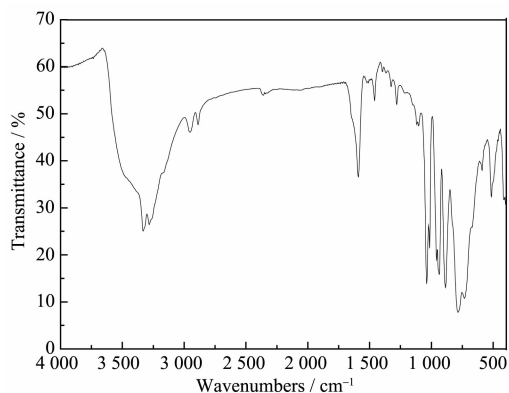
In the infrared spectra of **1** (Fig.3), four characteristic peaks at 1 035~1 014, 957~937, 889, 786~732  $\text{cm}^{-1}$  are attributed to the  $\nu_{\text{as}}(\text{P}-\text{O}_\text{a})$ ,  $\nu_{\text{as}}(\text{W}-\text{O}_\text{i})$ ,

Table 3 Selected parameters of hydrogen-bonds for the complex **1**

D-H...A	$d(\text{D-H}) / \text{nm}$	$d(\text{H}\cdots\text{A}) / \text{nm}$	$d(\text{D}\cdots\text{A}) / \text{nm}$	$\angle \text{DHA} / (^\circ)$
N1-H1A...O42' <sub>b</sub> <sup>v</sup>	0.090	0.247 9	0.326 3	145.8
N2-H2B...O38 <sup>v</sup>	0.090	0.232 8	0.310 4	144.31
N3-H3A...O16 <sup>iii</sup>	0.090	0.210 1	0.299 7	173.19
N4-H4B...O13 <sup>ix</sup>	0.090	0.219 2	0.299 0	147.36
N5-H5A...O38 <sup>v</sup>	0.090	0.230 5	0.317 5	162.31
N6-H6A...O13 <sup>ix</sup>	0.090	0.240 8	0.310 2	134.08
N7-H7A...O40 <sup>x</sup>	0.090	0.221 6	0.303 3	150.62
N8-H8A...O40 <sup>iii</sup>	0.090	0.220 1	0.301 4	150.01
N9-H9A...O9 <sup>v</sup>	0.090	0.244 0	0.312 3	132.96
N10-H10A...O31 <sup>xi</sup>	0.090	0.216 8	0.296 1	146.52
O35-H35B...O30 <sup>j</sup>	0.085	0.217 0	0.294 4	151.39
O36-H36B...O28 <sup>viii</sup>	0.085	0.200 0	0.280 5	157.85
O37-H37C...O44	0.085	0.194 4	0.279 4	179.2
O38-H38C...O11 <sup>v</sup>	0.085	0.218 6	0.302 1	167.25
O39-H39C...O12 <sup>v</sup>	0.085	0.213 6	0.298 6	177.99
O40-H40C...O37	0.085	0.216 5	0.301 5	179.2
O41-H41C...O39	0.085	0.225 9	0.310 3	171.86
O42-H42G_a...O5 <sup>v</sup>	0.085	0.228 8	0.312 4	168.15
O43-H43C...O7 <sup>iv</sup>	0.085	0.204 1	0.288 8	174.46
O44-H44E_a...O39 <sup>v</sup>	0.085	0.219 1	0.304 0	177.38

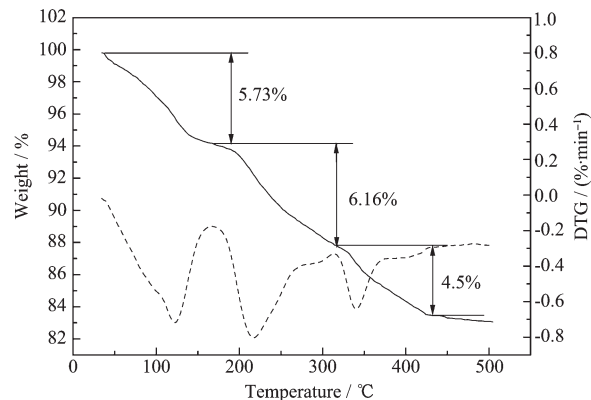
Symmetry code: <sup>i</sup>  $-x+1, -y+1, -z+1$ ; <sup>iv</sup>  $x, y+1, z$ ; <sup>v</sup>  $-x+1, -y+2, -z+1$ ; <sup>vii</sup>  $-x+2, -y+3, -z+1$ ; <sup>viii</sup>  $-x+1, -y+2, -z+2$ ; <sup>ix</sup>  $-x+2, -y+2, -z+2$ ; <sup>x</sup>  $x-1, y, z-1$ ; <sup>xi</sup>  $x+1, y+1, z$ .

$\nu_{\text{as}}(\text{W-O}_b\text{-W})$  and  $\nu_{\text{as}}(\text{W-O}_c\text{-W})$  stretching vibration, respectively. Compared with the typical Keggin-type  $\text{H}_3\text{PW}_{12}\text{O}_{40}$ <sup>[13]</sup>, the  $\text{P-O}_a$ ,  $\text{W-O}_b$  and  $\text{W-O}_c$  stretching vibration bands split into two bands as a consequence of the lower symmetry of the polyoxoanion. The characteristic peaks at 1 595, 1 459  $\text{cm}^{-1}$  in the complex **1** can be regarded as features of the bending vibration bands of  $-\text{NH}_2$  and  $-\text{CH}_2$  groups, the stretching bands of the  $-\text{NH}_2$  groups are observed at 3 332~3 277  $\text{cm}^{-1}$ .

Fig.3 IR spectrum of complex **1**

### 2.3 Thermal analysis

The TGA-DTG analysis for complex **1** was performed from 34 to 500  $^\circ\text{C}$  at a heating rate of 15  $^\circ\text{C} \cdot \text{min}^{-1}$  under nitrogen atmosphere. The results of TGA-DTG analysis curves in Fig.4 for **1** show a decomposition proceeds in a three-step fashion which shows three heat-absorption peaks located at 122, 218 and 341  $^\circ\text{C}$  respectively. The first process of weight loss of about 5.73% from 34 to 168  $^\circ\text{C}$  corresponded to the release of twenty water molecules (Calcd.

Fig.4 Thermal analysis curves for the complex **1**

6.05%). The second weight loss of about 6.16% (Calcd. 6.05%) from 168 to 314 °C attributed to the release of six en ligands. The third weight loss of about 4.5% (Calcd. 4.03%) between 314 and 432 °C assigned to the decomposition of four en ligands.

## 2.4 Cyclic voltammetric study

The cyclic voltammetry behavior of 1-CPE in HAc-NaAc buffer solution (pH=4) from -0.8~1.0 V with different scan rates was studied (Fig.5). The cyclic voltammetric data exhibit one redox pair which appears at  $E_{1/2}=0.089\text{ V}$  ( $E_{1/2}=(E_{pc}+E_{pa})/2$ , where  $E_{1/2}$  is the mean peak potentials,  $E_{pa}$  the anode peak potentials,  $E_{pc}$  the cathode peak potentials, scan rate  $80\text{ mV}\cdot\text{s}^{-1}$ ), corresponding the irreversible redox process of the nickel. When the scan rates varied from 80 to  $120\text{ mV}\cdot\text{s}^{-1}$  for the compound **1**, it is found that the cathodic peak potentials shift towards the negative direction and the anodic peak potentials towards the

positive direction. The peak currents are proportional to the scan rate, confirming the irreversible process for the compound **1** are surface-controlled.

## References:

- [1] Niu J Y, Wang K H, Chen H N, et al. *Cryst. Growth Des.*, **2009**,**9**:4362-4372
- [2] Mialane P, Dolbecq A, Marrot J, et al. *Chem. Eur. J.*, **2005**, **11**:1771-1778
- [3] Kortz U, Hussian F, Reicke M. *Angew. Chem. Int. Ed.*, **2005**,**44**:3773-3777
- [4] Mialane P, Dolbecq A, Sécheresse F. *Chem. Commun.*, **2006**, **33**:3477-3485
- [5] Sankarraj A V. *Thesis for the Doctorate of Auburn University*. **2008**.
- [6] Han Q X, Liu Y, Li J, et al. *Chiese J. Struct. Chem.*, **2009**, **28**:25-28
- [7] LI Xin-Xiong(李新雄), FANG Wei-Hui(芳伟慧), YANG Guo-Yu(杨国昱). *Chem. J. Chinese Universities(Gaodeng Xuexiao Huaxue Xuebao)*, **2011**,**32**:571-576
- [8] Wu J, Wang C X, Su Z H, et al. *Chinese J. Struct. Chem.*, **2012**,**31**:271-279
- [9] Li B, Zhao D, Zheng S T, et al. *J. Clust. Sci.*, **2008**,**19**:641-650
- [10] Sheldrick G M. *SHELXS-97, Program for Crystal Structure Solution*, University of Göttingen, Germany, **1997**.
- [11] Sheldrick G M. *SHELXL-97, Program for the Refinement of Crystal Structure*, University of Göttingen, Germany, **1997**.
- [12] Weakley T J R, Evans Jr H T, Showell J S, et al. *J. Chem. Soc. Chem. Commun.*, **1973**,**4**:139-140
- [13] Claud R D, Michael F, Raymonde F, et al. *Inorg. Chem.*, **1983**,**22**:207-216

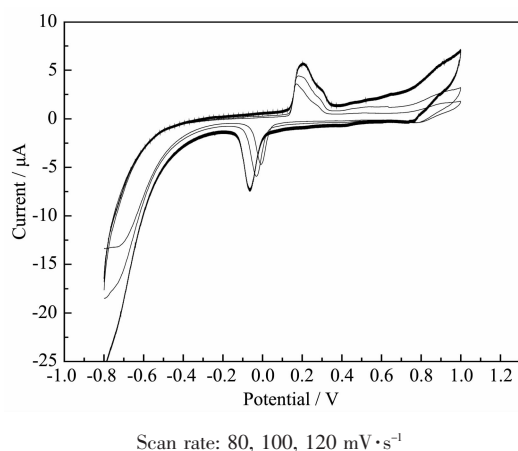


Fig.5 Cyclic voltammograms of the complex **1**